IEEE Access
Multidisciplinary | Rapid Review | Open Access Journal

Received April 29, 2019, accepted May 15, 2019, date of publication June 26, 2019, date of current version July 26, 2019.

Digital Object Identifier 10.1109/ACCESS.2019.2925049

Optimal Power Flow and Unified Control Strategy for Multi-Terminal HVDC Systems

ALI RAZA[1], ALI MUSTAFA[1], KUMARS ROUZBEHI[3], (Senior Member, IEEE), MOHSIN JAMIL[1], SYED OMER GILANI[1], GHULAM ABBAS[2], (Senior Member, IEEE), UMAR FAROOQ[4], AND MUHAMMAD NAEEM SHEHZAD[5]

[1]Department of Robotic and AI, National University of Sciences and Technology, Islamabad 44000, Pakistan
[2]Department of Electrical Engineering, The University of Lahore, Lahore 54000, Pakistan
[3]Department of Electrical Engineering, Universidad Loyola Andalucía, 41014 Seville, Spain
[4]Department of Electrical Engineering, University of the Punjab, Lahore 54590, Pakistan
[5]COMSATS Institute of Information and Technology, Lahore 54000, Pakistan

Corresponding authors: Ali Raza (i.will.rize@gmail.com) and Mohsin Jamil (engrdrmohsin@gmail.com)

ABSTRACT This paper presents an automation strategy for multi-terminal HVDC (MT-HVDC) systems combining a dc optimal power flow (dc OPF) routine and a unified reference controller (URC). In the presented automatic framework, the dc OPF algorithm is implemented at the power dispatch center (PDC) of the MT-HVDC system to find optimal reference operation points of the power converters to minimize the losses during the operation of the MT-HVDC grid and solves the contradiction between minimizing losses and preventing commutation failure. At the local control systems, the operating points of the voltage-source converter (VSC) stations are tuned based on the calculations executed in the PDC, which enables fast response to power fluctuation and ensures a stable dc voltage. However, if the communication between the two control layers is lost, the MT-HVDC grid remains stable based on the pre-defined V–P droop characteristics for the power converter stations till the connection establishes again, and a set of new operating points is generated and sent. The static and dynamic simulations conducted on the CIGRE B4 HVDC test grid establish the efficient and effective grid control performance with the proposed automation strategy. The analysis shows that the proposed control scheme achieves the desired minimum losses while, at the same time, satisfying the system constraints.

INDEX TERMS CIGRE B4 HVDC test system, DC optimal power flow, multi-terminal HVDC systems (MT-HVDC), power dispatch center (PDC), unified control strategy.

I. INTRODUCTION

Broad academic and industrial studies within the field of Multi-Terminal HVDC (MT-HVDC) systems/grids have been conducted worldwide [1]–[8]. More than 200 HVDC projects have been launched worldwide since 1951 [4]. Over the past two-decade, some HVDC applications have been expanded with multi-power converter stations in order to explore the first operational MT-HVDC systems [2], [3]–[6].

Significant benefits and application concepts have been recognized and proposed with regards to the MT-HVDC system/grid [5]–[7]. The MT-HVDC systems can serve as the most promising solution for the integration of harvested offshore wind power into onshore ac grids [8]. Moreover, MT-HVDC grids can facilitate construction of the European super grid [9]–[14].

The need for MT-HVDC grids and their rewards for future power systems are well established. Conversely, at the time of writing this paper, the knowledge on this subject is rare. Some suggestions for primary control of DC grid voltage have been described in [1], [5], [15]–[20] that present several advantages and disadvantages. However, the MT-HVDC grid development still requires significant research, specifically in relation to grid control and operation, and interaction with connected AC grids [21], [8]. It would not be easy to adjust/control the power flow via redacting the set-points of VSCs in HVDC grid. Thus, DC Optimal Power Flow is important to enable the congestion management, handling the power market requests, loop power flow control and to avoid the bottleneck of power transmission [22], [23]. Overloading

The associate editor coordinating the review of this manuscript and approving it for publication was Lin Zhang.

of DC-link may lead to its damage and may cause eventual cascaded failure of whole system [1].

The DC OPF would accomplish the MT-HVDC requirements; losses, reliability, cost and power flow control along with the DC link voltage control [6], [24]–[26]. In [27], a two-layer hierarchical control framework taking into account of VSC-HVDC stations and the extra Serial-Parallel DC Power Flow Controller (SPDC-PFC) station was proposed and investigated. One of the objectives here is to maximize the utilization of existing DC grids within their reliable and safe boundaries via unified reference control (URC). DC OPF, subject, has attracted researchers both from industry and academia. Even CIGRE working group WG B4-58 is inspired and devoted to analyze the techniques, feasibility and the devices for automatic power flow in MT-HVDC systems [28].

Inter-area oscillations, reliability and stability of MT-HVDC systems are expressed in terms of DC-link voltage stability [29], [30]. Dynamic performance and stability analysis of DC grids have been comprehensively studied in [31]–[33] and established that DC grid stability might be on risk because of instabilities originated from the connected weak ac grids, resonance generated in MT-HVDC, constant utility load and the addition of HVDC-CBs [32]. Despite the availability of several studies on this topic, there is a clear gap of research regarding detailed dynamic research/study of DC OPF in concern of a Unified Reference Controller (URC) and thus, its impacts on MT-HVDC systems to develop a strategy towards optimal operation.

This paper presents an automation strategy for MT-HVDC grids combining a DC Optimal Power Flow (DC OPF) routine and a Unified Reference Controller. In the presented automatic framework, DC OPF algorithm is implemented at the Power Dispatch Centre (PDC) of the Multi-Terminal VSC-HVDC grid to find optimum reference operation points of the VSCs taking in account the operational limitations and MT-HVDC grid loss minimization. The power flow algorithm used in this paper contains an optimization algorithm designed in [34] for transmission loss minimization. At the local control systems, operating points of the converters are tuned based on the calculations executed in PDC. URC is implemented in the local control of MT-HVDC systems as a step towards flexible operation and thus automation. Owing to the obligation of AC power systems, fixed frequency and voltage-frequency droop modes are implemented, which gives provision of operation mode transition. AC frequency support and DC-link voltage stabilization is the key feature of the proposed strategy. As a result, MT-HVDC grid would participate in stabilization of the AC system by inertia sharing among different interacted AC networks. However, if the communication between two control layers is dropped, the DC system remains stable based on the pre-defined droop characteristics for the converter stations till the connection is established again and a set of new operating points is generated and sent. Static and dynamic simulations conducted on the CIGRE B4 HVDC test grid demonstrate the effective control routine with the proposed automation approach.

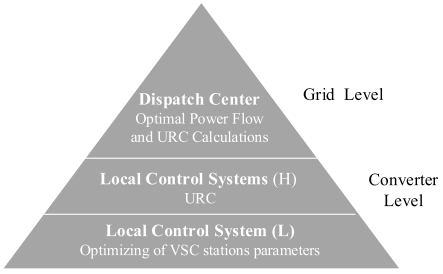

FIGURE 1. Proposed automation pyramid for MT-HVDC grid.

In this paper, a complete control-framework is presented in order to provide an efficient control and perform power-sharing in the MT-HVDC systems based on the DC OPF. This enables running at the supervisory control center and programming a Unified Reference Controller at the primary control of the VSC stations stepping towards the automation of MT-HVDC grids.

II. AUTOMATION APPROACH

Fig.1 illustrates the proposed automation framework in a pyramid form for MT-HVDC grid. The proposed framework has a hierarchical control structure that is comprised of power converter stations and grid control layers. To be clearer, low-level control of power converter stations is dedicated to the issues such as optimization of VSC-HVDC stations control parameters and the high-level control of the power converter level is devoted to the URC strategy. In the grid level, optimal power flow procedure and URC signal calculations are performed.

III. DISPATCH CENTER

DC optimal power flow is perceived as a limited version of the AC OPF, as reactive power (Q) is not available in MT-HVDC systems/grids.

Various objective functions can be defined for an OPF procedure [35], [36]. The problem of DC OPF to minimize the transmission losses in Multi-Terminal HVDC system is expressed by (1)-(5) considering an MT-HVDC system with N-DC buses. This can be expressed as follows:

$$f(V) = \min \left[\sum_{i=1}^{N} G_{ii} V_i^2 + \sum_{i=1}^{N} \sum_{j-(i+1)}^{N} G_{ij\cdot} \left(V_i - V_j\right)^2 \right] \quad (1)$$

where G_{ij}, is an element of the MT-HVDC grid's conductance matrix and P_{Gi} is the generations and P_{Li} is loads at the terminal i. N be the number of converter station/buses. And subject to the following equality and inequality constraints:

$$g(V, P) = 0 \quad (2)$$

$$|P_i| < P_i^{\max}, \quad i = 1, \ldots, N \quad (3)$$

$$V_{DC}^{\min} < V_{DC,i} < V_{DC}^{\max}, \quad i = 1, \ldots, N \quad (4)$$

$$\left|I_{DC,k}\right| < I_{DC,k}^{\max}, \quad k = 1, \ldots, M \quad (5)$$

where M is the number of transmission lines. Constraints (3)-(5) show the limitations of the Multi-Terminal VSC-HVDC system DC-link voltages, the power of the VSC-HVDC stations and the direct current through the transmission lines, respectively. P_i^{max}, in constraint (3), indicates the maximum permissible power of the i^{th} VSC. In (4), $V_{\mathrm{DC}}^{\min}$ and $V_{\mathrm{DC}}^{\max}$ designate the lower and upper bounds of DC-link voltages in MT-HVDC system, respectively. In (5), $I_{DC,k}^{max}$ is upper limit of the allowable direct current transferred by the k^{th} transmission line.

In (1), V is the vector of system's DC bus voltages:

$$V = [V_{DC.1}, V_{DC.2}, \ldots, V_{DC.N}]^T \tag{6}$$

The minimization function is:

$$f(V) = \sum_{i=1}^{N} G_{ii} V_i^2 + \sum_{i=1}^{N} \sum_{j=(i+1)}^{N} G_{ij} \left(V_i - V_j\right)^2 \tag{7}$$

The constraint expressed in (2) consist discrepancy between demand and generation which imposes in DC OPF equations, as following:

$$g\,(V, P) = [g_1, g_2, \ldots, g_N]^T \tag{8}$$

$$P = [P_1, P_2, \ldots, P_N]^T \tag{9}$$

Here, P denotes the vector of grid's powers:

$$g_i = \sum_{j=1}^{N} G_{ij} V_i V_j + P_{Gi} - P_{Mi} \tag{10}$$

The DC OPF problem stated in (1)-(5) is a nonlinear-constrained optimization problem which can be solved by the use of a gradient-based optimization technique, as:

$$L\,(V, P) = f\,(V) + q\,(V, P, I) + \lambda^T g\,(V, P) \tag{11}$$

Here, λ is a vector of Lagrange multipliers for the equality constraint presented by (12). I is the vector of direct currents flowing through DC transmission lines and q is the penalty function for the inequality constraints and defined by:

$$\begin{aligned} &q\,(V, P, I) \\ &= \sum_{i=1}^{N} \left\{ \begin{array}{l} \left(V_i - V_i^{\min}\right)^2 pf_{V^{\min},i} + \left(V_i - V_i^{\max}\right)^2 pf_{v^{\max},i} \\ + \left(P_i - P_i^{\max}\right)^2 pf_{P^{\max},i} \end{array} \right\} \\ &\quad + \sum_{k=1}^{L} \left(I_{DC,ki} - I_{DC,i}^{\max}\right)^2 pf_{I,k} \end{aligned} \tag{12}$$

where, $pf_{v^{\min},i}$, $pf_{v^{\max},i}$, $pf_{P^{\max},i}$, and $pf_{I,i}$ denote the penalty factors for minimum and maximum limits of DC-link voltage, power converter stations limits, and transmission lines limits, respectively [35].

The result of the DC OPF will be achieved by equating the Lagrangian derivative with respect to the unknown variables to zero, and then to solve the problem iteratively:

$$\frac{\partial L}{\partial V} = \frac{\partial q}{\partial V} + \frac{\partial f}{\partial V} + \left[\frac{\partial g}{\partial V}\right]^T \lambda \tag{13}$$

$$\frac{\partial L}{\partial \lambda} = g\,(V, P) \tag{14}$$

IV. LOCAL CONTROLLERS

With the ability of switching between the VSC-HVDC stations operational modes, grid will automatically deal with the perturbations in loads and primary sources and, even go through the fault contingencies. Fig. 2 demonstrates the control structure of the VSC-HVDC stations, regarded as URC. This control structural design is anticipated as a unified technique to control and operate VSC-HVDC stations in MT-HVDC systems. The control layers, inner current controller and the outer controllers as shown in Fig. 2(a) are identical to the classic control arrangements of VSC-HVDC station.

The detailed layout of the URC is presented in Fig. 2(b). P_{set} is an active power mandate set by the DC OPF algorithm, and A_{K} is a parameter matrix given in (15). K_{Pf} is proportional gain for frequency control, K_{If} is integral gain for frequency control, K_{Pu} is proportional gain for voltage control, and K_{Iu} is integral gain for voltage control as shown in Fig. 2(b).

$$A_K = \begin{bmatrix} K_{pf} & K_{If} \\ K_{pu} & K_{Iu} \end{bmatrix} \tag{15}$$

The elements of $\mathrm{A_K}$ matrix are decided in PDC contains an optimization algorithm designed in [34]. The URC can be used for all the VSC stations, and the role of each station can be simply assigned or changed via 'control order settings for URCs' in PDC. The elements of $\mathrm{A_K}$ may be zero or non-zero during various control modes, but it should always have zero elements to evade from the control fighting. With the distinct arrangement of $\mathrm{A_K}$, the URC accomplishes various functions, thus allocate the necessary operation mode to the controlled VSC station. Moreover, for operation modes like f or V_{DC} control, P_{set} should be set to zero. T_{tr} is the transition time, and the gain scheduling block will adjust $\mathrm{A_K}$ to the objective during the transition time. The grid operation modes is chosen and generalized as follows:

Frequency control: $K_{Pf} \neq 0, K_{If} \neq 0, K_{Pu} = 0, K_{Iu} = 0$.

$$P_{ref} = \left(K_{Pf} + \frac{K_{If}}{s}\right)\left(f_{ref} - f\right) \tag{16}$$

P-V_{DC} droop control: $K_{Pf} = 0$, $K_{If} = 0$, $K_{Pu} \neq 0$, $K_{Iu} = 0$.

$$P_{ref} = P_{set} + K_{pu}(V_{DC} - V_{DC\_ref}) \tag{17}$$

V_{DC} control: $K_{Pf} = 0, K_{If} = 0, K_{Pu} \neq 0, K_{Iu} \neq 0$.

$$P_{ref} = \left(K_{pu} + \frac{K_{Iu}}{s}\right)\left(V_{DC} - V_{DC\_ref}\right) \tag{18}$$

P-f droop control: $K_{Pf} \neq 0, K_{If} = 0, K_{Pu} = 0, K_{Iu} = 0$.

$$P_{ref} = P_{set} + K_{pf}(f_{ref} - f) \tag{19}$$

V_{DC}-f control: $K_{Pf} \neq 0, K_{If} = 0, K_{Pu} \neq 0, K_{Iu} = 0$.

$$P_{ref} = P_{set} + K_{pf}(f_{ref} - f) + K_{pu}(V_{DC} - V_{DC\_ref}) \tag{20}$$

In order to switch to fixed power mode, K_{Pf}, K_{If}, K_{Pu}, and K_{Iu} should set to zero.

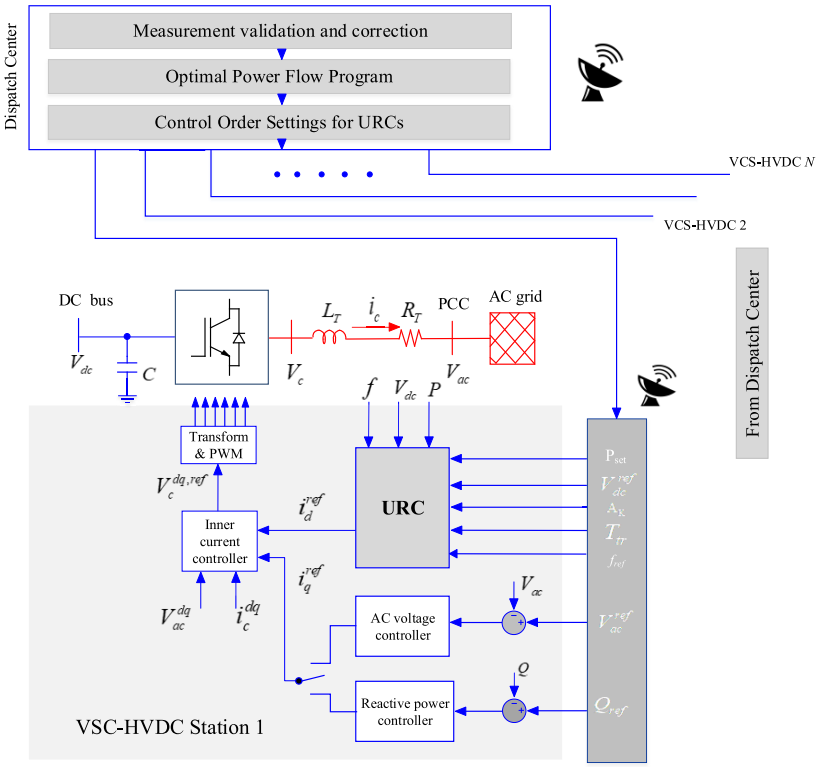

(a)**General control architecture**

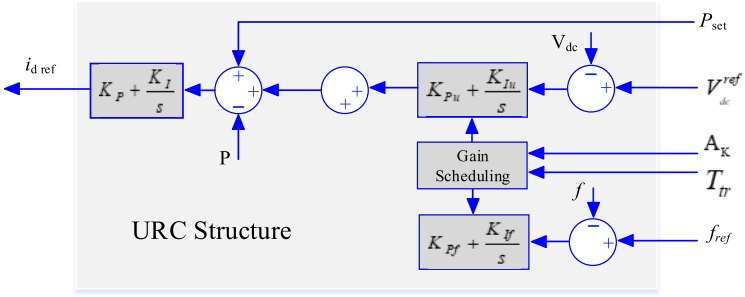

(b) The unified reference controller

FIGURE 2. **Local control for VSC stations.**

V. AC-DC INTERACTION AND INERTIA SHARING

So far, MT-HVDC systems simply play the role of an energy corridor for AC grids, and mostly the issues related to the control and operation of DC side are investigated. AC-DC interaction and inertia sharing means to increase the inertia of an island/weak AC system. An AC grid can be considered as a weak grid from two points of views: first, high AC-grid impedance [37] and second, low AC-generation inertia. Normally, inertia emulation control is developed by regulating DC grid voltage following the AC frequency in a specified trajectory based on the inertia characteristics and the energy stored on the DC bus acts as inertia reserve [38], [39]. With reference to the suggested URC, the perturbations from AC grid will also be handsomely managed. It means that fluctuations from AC side will alter the MT-HVDC grid voltages and hence affect the frequencies of other connected AC networks.

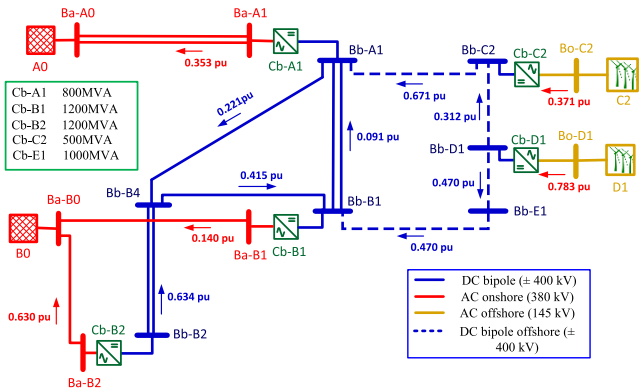

FIGURE 3. **CIGRE B4 DCS3 five terminal HVDC grid test system.**

Coupling dynamics give provision to share strength of stiff areas to mitigate the disturbances in overall network. On the other hand, it may propagate the perturbations in the system

TABLE 1. Transmission lines data.

Line Data	Length	R [Ω/km]	L [mH/km]	C [μF/km]	G [μS/km]
OHL (DC)	900km	0.0114	0.9356	0.0123	0.000
OHL (AC)	600km	0.0200	0.8532	0.0135	0.000
Cable (DC)	900km	0.0095	2.1120	0.1906	0.048
Cable (AC)	150km	0.0184	2.5729	0.2315	0.059

TABLE 2. VSC stations parameters.

VSC station	R (Ω)	L (mH)	C (μF)
Cb-A1	0.403	33	450
Cb-B1	0.403	33	450
Cb-B2	0.403	33	450
Cb-C2	1.210	98	150
Cb-D1	0.650	49	300

TABLE 3. DC OPF results of the steady state base-case.

DC bus	DC voltage (pu)	Net power (pu)
Bb-C2	1.012	+0.371
Bb-D1	1.013	+0.783
Bb-E1	1.016	-0.470
Bb-A1	1.015	-0.671
Bb-B1	1.014	-0.091
Bb-B2	1.007	+0.634
Bb-B4	1.011	-0.415

and even cause instability. The second situation needs to be evaded via right control design. This topic is covered in details in [40].

VI. SIMULATION RESULTS

The proposed control framework is evaluated considering CIGRE B4 DCS3 Multi-Terminal VSC-HVDC systems [41]. As shown in Fig. 3, the test system is a 5-terminal bipolar meshed VSC-HVDC grid, engaged to assess the anticipated automation control strategy. The base power and DC voltage for normalization are 1200 MVA and 400 kV, respectively.

Electrical data of DC transmission lines and converter stations parameters are given in Tables 1 and 2, respectively. L and R are total inductance and resistance between AC grid and the VSC-HVDC converter while C is the capacitance of DC bus in Table 2.

Simulation results are presented to confirm the effectiveness of the projected DC OPF control and dynamic interaction between AC and DC grids during base case, deficiency in power generation in weak AC network and ultimate breakage of transmission line.

A. STATIC SIMULATION OF THE BASE-CASE

Static base-case simulation based on DC OPF data is given in Table 3. Due to omitting the DC transmission losses in this figure, sum of the incoming and outgoing power at buses deviate from zero. Slack converter Cb-B1 has least droop slope. Thus, it has largest contribution to power sharing and DC grid voltage control.

B. GENERATION DEFICIENCY IN WEAK AC GRID

Firstly, event E_A is triggered in which one of the synchronous machines within weak AC grid A0 loses its 200 MW power

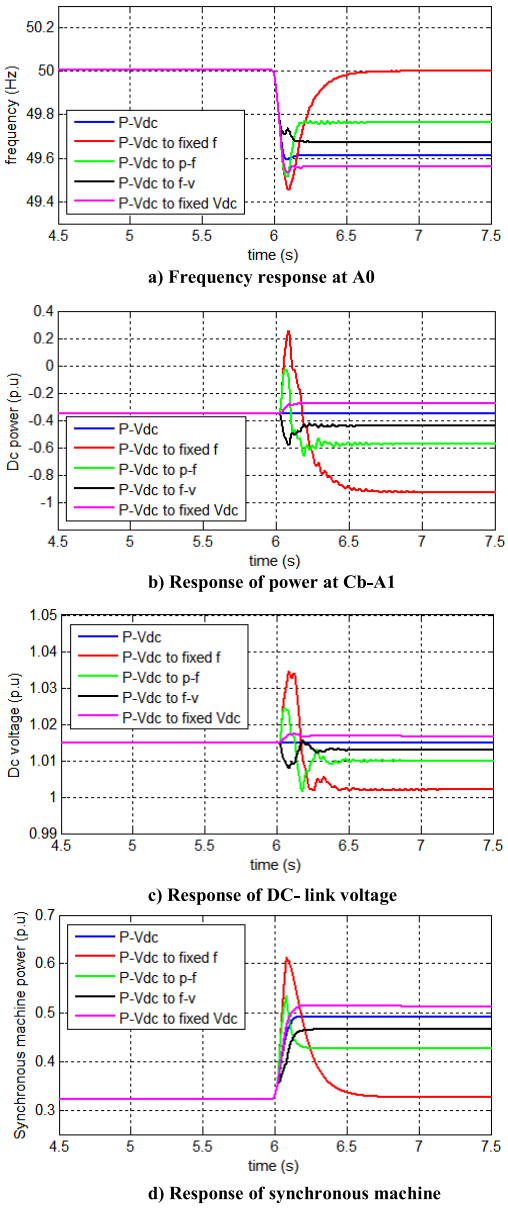

FIGURE 4. MT-HVDC grid response to deficiency in power generation.

under P-V_{DC} droop control mode because of sudden loss in mechanical power. Fig. 4 shows that the other generator in A0 raises its yield to maintain power equilibrium. Since the frequency is dropped due to loss of generation, VSC-HVDC station tries to increase its power injection to stabilize the system frequency, accompanied with the fall in DC-link voltage at Ba-A1. For such a scenario, the proposed URC control would automatically shift to stabilize the frequency, voltage and power profiles via DC OPF algorithm implemented in dispatch center. Results based on different control modes of URC are shown in Fig. 4 and numerically tabulated in Table 4. Optimal reference operation points of the VSCs are found using (7) to minimize the operational losses by avoiding commutation failure, as achieved in Fig. 2. It is clear in Fig. 4 that control transition from P-V_{DC} droop to P-f

droop shows significant performance than other three control shifting setups with minimized losses.

For instance, although it seems from Fig. 4 that fixed-f transition (50 Hz) shows better frequency response than P-f (49.76 Hz) droop control but overall response is not promising. As each employed VSC have specific power transfer capability. Fixed-f shows better frequency response but the power drawn by the converter is much higher (0.9275 pu) than the converter rating which may damage the VSC converter. Similarly, the DC-link voltage stabilizing time is longer under the fixed-f than P-f droop transition. The P-f droop control also improves the frequency response which is under the safe limitation ($\pm 1\%$ of nominal value) and at the same time power carrying capability is not violated. P-f droop transition (49.76 Hz) also shows better frequency response than f-V_{DC} transition (49.621 Hz) as depicted in Fig. 4.

During P-f droop control, the power flow through Cb-A1 increases to compensate DC-link voltage via Cb-B1 as shown in Fig. 3 and Fig. 4, respectively. Converter station Cb-B1 and Cb-B2 increase its injected power to 0.397 pu and 0.547 pu, respectively, with no change in imported power from Cb-C2 and Cb-D1 (i.e. 0.3712 pu and 0.7830 pu), respectively. VSCs connected with the strong AC grid B0, having stiff frequency are not affected with E_A. And thus, the frequency of weak AC grid A0 becomes stable as it receives inertia support from VSC Cb-A1 that is connected with Cb-B1 and Cb-B2, which are further linked with strong AC grid B0. Hence, B0 shares inertia with A0.

By comparing different control modes profiles in each scope of Fig. 4 and numerical data of Table 4, it is established that AC system supporting effect, power flow and DC-link voltages are improved along with minimization of transmission losses via proposed DC OPF routine and URC implementation. Prominently, DC voltage and power profiles after event E_A are still closely matching with DC OPF results of the base case.

C. BREAKAGE OF TRANSMISSION LINE

Event E_B, breakage of transmission line, is experienced on one of the two paralleled transmission lines (TLs) connecting Ba-A1 and Ba-A0 under *P-*V_{DC} droop control, resulting in total loss of TL and hence power transfer is lost. As the reactance of the line instantly increases and thus the power injected and supplied by both VSC Cb-A1 and synchronous machines of A0 rapidly decreases, resulting in the transients in frequency of A0 and DC voltage at Cb-A1. Thus, remaining transmission line becomes overloaded. Proposed OPF control for MT-HVDC is designed to deal with such an uncertain behavior of the system automatically.

At the local control systems, the operating points of the converter stations are tuned based on the calculations executed in the PDC, which enables fast response to power fluctuation and ensures a stable DC voltage. The trade-off between AC frequency and DC voltage supports is shown in Fig. 5 and numerically expressed in Table 5 based on the optimized reference control parameters of the URC.

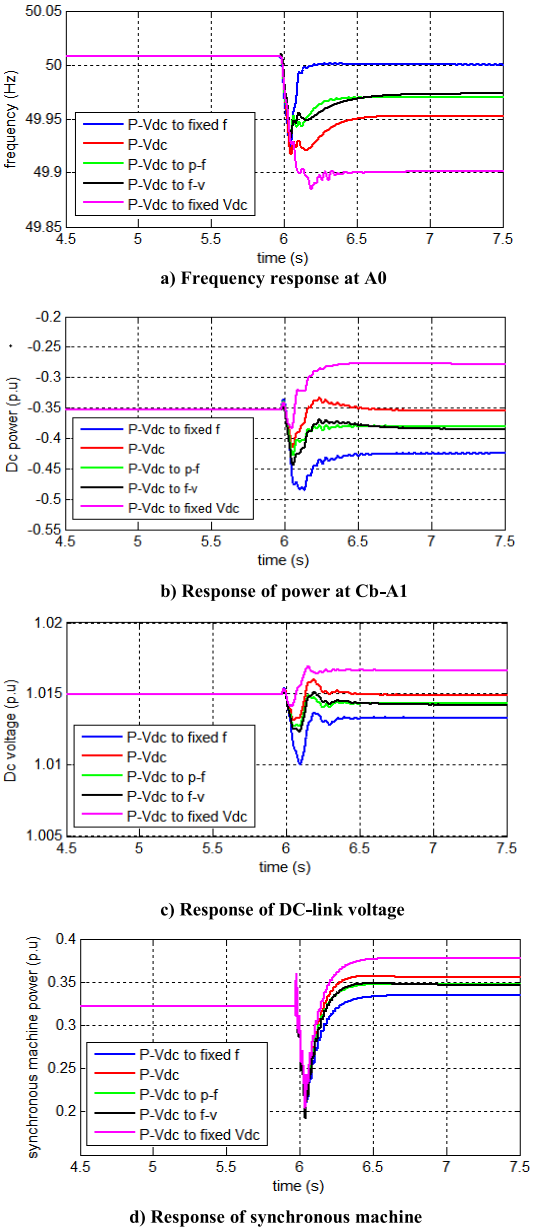

FIGURE 5. MT-HVDC grid response to breakage of transmission line.

The control would then modify itself to stabilize the frequency, DC voltage, and power flow. Frequency response is improved and transients are lowered for better power quality. Simulations proved that MT-HVDC system shows decent response (fast settling time) for a shift in *P-*V_{DC} droop to *P-f* droop control than other three controls shift as shown in Fig. 5 (a, b, c, d) under the same circumstances by achieving minimization loss.

The operation and control of CIGRE B4 DCS3 MT-HVDC grid test system under all three test scenarios show that the designed control and operation strategy combining a DC OPF routine and a Unified Reference Controller is effective. Minimization of transmission losses achieved by executing the DC OPF in supervisory control to find optimal reference operation points of VSCs. Results clearly show that the weak

TABLE 4. Numerical results of MT-HVDC grid response to deficiency in power generation.

	P-V_{DC} (49.6148 Hz)		P- V_{DC} to Fixed f (50 Hz)		P- V_{DC} to P-f (49.7641 Hz)	
DC bus	DC voltage (pu)	Net power (pu)	DC voltage (pu)	Net power (pu)	DC voltage (pu)	Net power (pu)
Bb-C2	1.017	+0.3710	1.005	+0.3712	1.013	+0.3712
Bb-D1	1.018	+0.7830	1.006	+0.7830	1.013	+0.7830
Bb-E1	1.016	-0.4704	1.004	-0.2992	1.012	-0.4044
Bb-A1	1.015	-0.3532	1.002	-0.9275	1.010	-0.5747
Bb-B1	1.014	-0.3237	1.003	-0.5143	1.010	-0.3970
Bb-B2	1.007	-0.6285	0.997	-0.4182	1.003	-0.5475
Bb-B4	1.011	+0.6309	1.001	+0.4192	1.007	+0.5493

	P- V_{DC} to Fixed V_{DC} (49.5980 Hz)		P- V_{DC} to f-V_{DC} (49.6213 Hz)	
DC bus	DC voltage (pu)	Net power (pu)	DC voltage (pu)	Net power (pu)
Bb-C2	1.016	+0.3712	1.016	+0.3712
Bb-D1	1.018	+0.7830	1.016	+0.7830
Bb-E1	1.016	-0.4779	1.014	-0.4441
Bb-A1	1.015	-0.3284	1.013	-0.4414
Bb-B1	1.015	-0.3156	1.013	-0.3528
Bb-B2	1.007	-0.6376	1.006	-0.5962
Bb-B4	1.011	+0.6400	1.009	+0.5984

TABLE 5. Numerical results of MT-HVDC grid response to breakage of transmission line.

	P-V_{DC} (49.952 Hz)		P-V_{DC} to Fixed f (50 Hz)		P-V_{DC} to P-f (49.970 Hz)	
DC bus	DC voltage (pu)	Net power (pu)	DC voltage (pu)	Net power (pu)	DC voltage (pu)	Net power (pu)
Bb-C2	1.017	+0.3712	1.016	+0.3712	1.017	+0.3712
Bb-D1	1.018	+0.7830	1.016	+0.7830	1.017	+0.7830
Bb-E1	1.016	-0.4700	1.015	-0.4490	1.015	-0.4624
Bb-A1	1.015	-0.3544	1.015	-0.4252	1.014	-0.3801
Bb-B1	1.014	-0.3241	1.013	-0.3475	1.014	-0.3325
Bb-B2	1.007	-0.6280	1.006	-0.6022	1.006	-0.6187
Bb-B4	1.011	+0.6304	1.009	+0.6004	1.010	+0.6210

	P-V_{DC} to Fixed V_{DC} (49.91 Hz)		P-V_{DC} to f-V_{DC} (49.973 Hz)	
DC bus	DC voltage (pu)	Net power (pu)	DC voltage (pu)	Net power (pu)
Bb-C2	1.019	+0.3712	1.017	+0.3712
Bb-D1	1.019	+0.7830	1.017	+0.7830
Bb-E1	1.017	-0.4911	1.015	-0.4609
Bb-A1	1.016	-0.2841	1.014	-0.3852
Bb-B1	1.016	-0.3009	1.014	-0.3342
Bb-B2	1.008	-0.6537	1.006	-0.6168
Bb-B4	1.012	+0.6563	1.010	+0.6191

AC grids receive decent inertia sharing and DC-link voltage and, power flow are upgraded by means of the proposed control approach based on DC OPF and URC.

VII. CONCLUSIONS

In this paper an optimal operation and unified control strategy for efficient and effective control and, power-sharing in MT-HVDC grids is proposed. In the anticipated control technique, a DC OPF procedure was implemented at the grid dispatch center. Then, at the local control systems, parameters of the unified control strategy were tuned based on the DC OPF which results in the operating point of the MT-HVDC grid, to provide an optimal operation of the MT-HVDC system to minimize the transmission losses and solves the conflict between minimizing losses and preventing commutation failure.

Dynamic simulations of five-terminal CIGRE B4 DCS3 MT-HVDC grid test system are developed in Simulink/MATLAB to extol the merits of the presented automatic control strategy. The simulated workbench was assessed for: (i) normal conditions (ii) deficiency in power generation in a weak AC grid (iii) breakage of a transmission line. Simulation results proof that the proposed DC OPF routine and URC implementation show significant improvement in AC grid supporting effect (inertia sharing), DC power flow and DC-link voltages regulation during both steady and dynamic states by achieving desired minimum losses. Further, simulations established that MT-HVDC grid profiles well match with test (i) base case DC OPF results during both test (ii) and (iii), respectively.

REFERENCES

[1] A. Raza, X. Dianguo, L. Yuchao, S. Xunwen, B. W. Williams, and C. Cecati, "Coordinated operation and control of VSC based multiterminal high voltage DC transmission systems," *IEEE Trans. Sustain. Energy*, vol. 7, no. 1, pp. 364–373, Jan. 2016.

[2] K. Meah and A. H. M. S. Ula, "A new simplified adaptive control scheme for multi-terminal HVDC transmission systems," *Int. J. Elect. Power Energy Syst.*, vol. 32, no. 4, pp. 243–253, May 2010.

[3] *Atlantic Wind Connection*. Accessed: Sep. 20, 2018. [Online]. Available: www.atlanticwindconnection.com

[4] K. Rouzbehi, A. Miranian, J. L. Candela, A. Luna, and P. Rodriguez, "A generalized voltage droop strategy for control of multiterminal DC grids," *IEEE Trans. Ind. Appl.*, vol. 51, no. 1, pp. 607–618, Jan./Feb. 2015.

[5] K. Rouzbehi, A. Miranian, A. Luna, and P. Rodriguez, "Optimized control of multi-terminal DC grids using particle swarm optimization," *EPE J.*, vol. 24, no. 2, pp. 38–49, 2014.

[6] K. Rouzbehi, A. Miranian, J. I. Candela, A. Luna, and P. Rodriguez, "Proposals for flexible operation of multi-terminal DC grids: Introducing flexible DC transmission system (FDCTS)," in *Proc. Int. Conf. Renew. Energy Res. Appl. (ICRERA)*, Oct. 2014, pp. 180–184.

[7] C. Dierckxsens, K. Srivastava, M. Reza, S. Cole, J. Beerten, and R. Belmans, "A distributed DC voltage control method for VSC MTDC systems," *Electr. Power Syst. Res.*, vol. 82, pp. 54–58, Jan. 2012.

[8] D. Van Hertem and M. Ghandhari, "Multi-terminal VSC HVDC for the European supergrid: Obstacles," *Renew. Sustain. Energy Rev.*, vol. 14, no. 9, pp. 3156–3163, Dec. 2010.

[9] L. Xu, B. W. Williams, and L. Yao, "Multi-terminal DC transmission systems for connecting large offshore wind farms," in *Proc. IEEE Power Energy Soc. Gen. Meeting-Convers. Del. Elect. Energy 2st Century*, Jul. 2008, pp. 1–7.

[10] R. da Silva, R. Teodorescu, and P. Rodriguez, "Multilink DC transmission system for supergrid future concepts and wind power integration," in *Proc. IET RPG*, 2011, pp. 1–6.

[11] L. Weimers, "A European DC super grid—A technology providers view," ABB, Brussels, Belgium, Tech. Rep., 2011.

[12] J. Dai, Y. Phulpin, A. Sarlette, and D. Ernst, "Coordinated primary frequency control among non-synchronous systems connected by a multi-terminal high-voltage direct current grid," *IET Gener., Transmiss. Distrib.*, vol. 6, no. 2, pp. 99–108, 2012.

[13] S.-Y. Ruan, G.-J. Li, X.-H. Jiao, Y.-Z. Sun, and T. T. Lie, "Adaptive control design for VSC-HVDC systems based on backstepping method," *Electr. Power Syst. Res.*, vol. 77, nos. 5–6, pp. 559–565, 2007.

[14] B. K. Johnson, R. H. Lasseter, F. L. Alvarado, and R. Adapa, "Expandable multiterminal DC systems based on voltage droop," *IEEE Trans. Power Del.*, vol. 8, no. 4, pp. 1926–1932, Oct. 1993.

[15] K. Rouzbehi, A. Miranian, J. I. Candela, A. Luna, and P. Rodriquez, "A novel approach for voltage control of multi-terminal DC grids with offshore wind farms," in *Proc IEEE ECCE Asia*, Melbourne, VIC, Australia, Jun. 2013, pp. 965–970.

[16] K. Rouzbehi, A. Miranian, A. Luna, and P. Rodriquez, "A generalized voltage droop strategy for control of multi-terminal DC grids," in *Proc. IEEE ECCE Asia*, Denver, CO, USA, Sep. 2013, pp. 59–64.

[17] N. R. Chaudhuri and B. Chaudhuri, "Adaptive droop control for effective power sharing in multi-terminal DC (MTDC) Grids," *IEEE Trans. Power Syst.*, vol. 28, no. 1, pp. 21–29, Feb. 2013.

[18] T. K. Vrana, J. Beerten, R. Belmans, and O. B. Fosso, "A classification of DC node voltage control methods for HVDC grids," *Electr. Power Syst. Res.*, vol. 103, pp. 137–144, Oct. 2013.

[19] J. Zhu, *Optimization of Power System Operation*. Hoboken, NJ, USA: Wiley, 2009.

[20] K. Rouzbehi, W. Zhang, J. Ignacio Candela, A. Luna, and P. Rodriguez, "Unified reference controller for flexible primary control and inertia sharing in multi-terminal voltage source converter-HVDC grids," *IET Gener., Transmiss. Distrib.*, vol. 11, no. 3, pp. 750–758, Sep. 2016.

[21] P. Rodriguez and K. Rouzbehi, "Multi-terminal DC grids: Challenges and prospects," *J. Mod. Power Syst. Clean Energy*, vol. 5, no. 4, pp. 515–523, 2017.

[22] J. Sau-Bassols, E. Prieto-Araujo, and O. Gomis-Bellmunt, "Modelling and control of an interline current flow controller for meshed HVDC grids," *IEEE Trans. Power Del.*, vol. 32, no. 1, pp. 11–22, Feb. 2017.

[23] Z. Li, Y. Li, R. Zhan, Y. He, and X.-P. Zhang, "AC grids characteristics oriented multi-point voltage coordinated control strategy for VSC-MTDC," *IEEE Access*, vol. 7, pp. 7728–7736, 2019.

[24] K. Rouzbehi, J. I. Candela, A. Luna, G. B. Gharehpetian, and P. Rodriguez, "Flexible control of power flow in multiterminal DC grids using DC-DC converter," *IEEE J. Emerg. Sel. Topics Power Electron.*, vol. 4, no. 3, pp. 1135–1144, Sep. 2016.

[25] A. Raza, L. Yuchao, K. Rouzbhehi, M. Jamil, S. O. Gilani, X. Dianguo, and B. W. Williams, "Power dispatch and voltage control in multi-terminal HVDC systems: A flexible approach," *IEEE Access*, vol. 5, pp. 24608–24616, 2017.

[26] K. Rouzbehi, A. Miranian, J. I. Candela, A. Luna, and P. Rodriguez, "A hybrid power flow controller for flexible operation of multi-terminal DC grids," in *Proc. Int. Conf. Renew. Energy Res. Appl. (ICRERA)*, Oct. 2014, pp. 550–555.

[27] K. Rouzbehi, S. S. H. Yazdi, and N. S. Shariati, "Power flow control in multi-terminal HVDC grids using a serial-parallel DC power flow controller," *IEEE Access*, vol. 6, pp. 56934–56944, 2018.

[28] (2016). *Devices for Load flow Control and Methodologies for Direct Voltage Control in a Meshed HVDC Grid*. [Online]. Available: http://b4.cigre.org/

[29] S. S. H. Yazdi, K. Rouzbehi, J. I. Candela, J. Milimonfared, and P. Rodriguez, "Flexible HVDC transmission systems small signal modelling: A case study on CIGRE Test MT-HVDC grid," in *Proc. 43rd Annu. Conf. IEEE Ind. Electron. Soc. IECON*, Beijing, China, Oct./Nov. 2017, pp. 256–262.

[30] S. S. H. Yazdi, J. Milimonfared, S. H. Fathi, and K. Rouzbehi, "Optimal placement and control variable setting of power flow controllers in multi-terminal HVDC grids for enhancing static security," *Int. J. Elect. Power Energy Syst.*, vol. 102, pp. 272–286, Nov. 2018.

[31] G. Pinares and M. Bongiorno, "Analysis and mitigation of instabilities originated from DC-side resonances in VSC-HVDC systems," *IEEE Trans. Ind. Appl.*, vol. 52, no. 4, pp. 2807–2815, Apr. 2016.

[32] W. Wang, M. Barnes, O. Marjanovic, and O. Cwikowski, "Impact of DC breaker systems on multiterminal VSC-HVDC stability," *IEEE Trans. Power Del.*, vol. 31, no. 2, pp. 769–779, Apr. 2016.

[33] Y. Liu, A. Raza, K. Rouzbehi, B. Li, D. Xu, and B. W. Williams, "Dynamic resonance analysis and oscillation damping of multiterminal DC grids," *IEEE Access*, vol. 5, pp. 16974–16984, 2017.

[34] K. Rouzbehi, A. Miranian, A. Luna, and P. Rodriguez, "DC voltage control and power sharing in multiterminal DC grids based on optimal DC power flow and voltage-droop strategy," *IEEE J. Emerg. Sel. Topics Power Electron.*, vol. 2, no. 4, pp. 1171–1180, Dec. 2014.

[35] T. M. Haileselassie, R. E. Torres-Olguin, T. K. Vrana, K. Uhlen, and T. Undeland, "Main grid frequency support strategy for VSC-HVDC connected wind farms with variable speed wind turbines," in *Proc. IEEE PowerTech*, Trondheim, Norway, Jun. 2011, pp. 1–6.

[36] A. K. Marten and D. Westermann, "Load frequency control in an interconnected power system with an embedded HVDC grid," in *Proc. IEEE PES Gen. Meeting*, San Diego, CA, USA, Jul. 2012, pp. 1–7.

[37] A. Martinez, "Connecting wind power plant with weak grid," Vestas Wind Syst., Denmark, Tech. Rep. 26, Mar. 2015.

[38] J. Zhu, C. D. Booth, G. P. Adam, A. J. Roscoe, and C. G. Bright, "Inertia emulation control strategy for VSC-HVDC transmission systems," *IEEE Trans. Power Syst.*, vol. 28, no. 2, pp. 1277–1287, May 2013.

[39] J. Zhu, J. M. Guerrero, W. Hung, C. D. Booth, and G. P. Adam, "Generic inertia emulation controller for multi-terminal voltage-source-converter high voltage direct current systems," *IET Renew. Power Gener.*, vol. 8, no. 7, pp. 740–748, 2014.

[40] W. Zhang, K. Rouzbehi, A. Luna, G. B. Gharehpetian, and P. Rodriguez, "Multi-terminal HVDC grids with inertia mimicry capability," *IET Renew. Power Gener.*, vol. 10, no. 6, pp. 752–760, 2016.

[41] *CIGRE B4 Working Group*. Accessed: Sep. 19, 2015. [Online]. Available: http://b4.cigre.org/publications

ALI RAZA received the B.S. and M.Sc. degrees in electrical engineering from the University of Engineering and Technology, Lahore, Pakistan, in 2010 and 2013, respectively, and the Ph.D. degree in electrical engineering from the Harbin Institute of Technology, Harbin, China, in 2016.

He is currently an Assistant Professor with the Department of Robotics and AI, National University of Sciences and Technology (NUST), Pakistan, and the Department of Electrical Engineering, The University of Lahore, Pakistan. He has authored or coauthored several technical journal papers and technical conference proceedings. His research interests include operation and control of M-VSC-HVDC, including its effects on power systems, protection, optimization, and topological evaluation of MT-HVDC transmission systems for large offshore wind power plants. He has been a TPC Member of the International Symposium on Wireless Systems and Networks (ISWSN), since 2017. He received the First Best Paper Award at the 2014 IEEE International Conference on Control Science and Systems Engineering. He is also the Co-Chair of the Asia Pacific International Conference on Electrical Engineering 2019 (APICEE 2019).

ALI MUSTAFA was born in Khanpur, Pakistan, in 1992. He received the M.Sc. degree in electrical engineering from The University of Lahore (UOL), Lahore, Pakistan, in 2018. He is currently a Lecturer with the Department of Robotics and AI, National University of Sciences and Technology (NUST), Pakistan, and the Department of Electrical Engineering, UOL. His research interests include the application of power electronics in power systems and multi-terminal HVDC systems.

KUMARS ROUZBEHI received the Ph.D. degree in electric energy systems from the Technical University of Catalonia (UPC), Barcelona, Spain. Prior to the Ph.D. program, he was with the Faculty of Electrical Engineering, Islamic Azad University (IAU), from 2004 to 2011, where he became the Director of the Department of Electrical Engineering. In parallel with teaching and research at the IAU, he was the CEO of Khorasan Electric and Electronics Industries Researches Company, from 2004 to 2010. He is currently an Associate Professor with the Universidad Loyola Andalucía. He holds a patent in ac grid synchronization of voltage-source converters and has authored or coauthored several technical books, journal papers, and technical conference proceedings. He has been a TPC Member of the International Conference on Electronic, Communication, Control and Power Engineering (EEE-ECCP), since 2014, and a Scientific Board Member of the (IEA) International Conference on Technology and Energy Management, since 2015. He has been a member of the Amvaj-e-bartar Policy Making Committee. He received the Second Best Paper Award of the IEEE JOURNAL OF EMERGING AND SELECTED TOPICS IN POWER ELECTRONICS from the IEEE Power Electronics Society, in 2015. He has been serving as an Editor, since 2006. He serves as an Associate Editor of *IET High Voltage* and *IET Energy Systems Integration*.

MOHSIN JAMIL received the B.Eng. degree in industrial electronics from NED University, Pakistan, in 2004, the M.Sc. degree in electrical engineering from Dalarna University, Sweden, in 2006, and the Ph.D. degree from the University of Southampton, U.K., in 2011. He is currently an Assistant Professor with the Department of Robotics and AI, National University of Sciences and Technology (NUST), Islamabad, Pakistan. He is author of a book chapter and several IEEE publications. His research interests include control design, multi-terminal HVDC transmission systems, soft-switching techniques, and smart grid technologies.

SYED OMER GILANI received the M.Sc. degree in computer engineering from Sweden, in 2006, and the Ph.D. degree in electrical and computer engineering from the National University of Singapore, in 2013. From 2006 to 2008, he was with the Interactive Multimedia Lab, Singapore. He is currently an Assistant Professor with the National University of Sciences and Technology (NUST), Pakistan. His research interests include use of power electronic in power systems, multi-terminal HVDC transmission systems, human–machine interaction and networking, and active consult for industry on various projects.

GHULAM ABBAS received the B.E. degree from the University of Engineering and Technology, Lahore, Pakistan, in 2004, and the M.E. and Ph.D. degrees from the Institut National des Sciences Appliquées de Lyon, France, in 2008 and 2012, respectively, all in electrical engineering. He is currently with the Department of Electrical Engineering, The University of Lahore, Pakistan. He has published a number of papers in various IEEE conferences and international journals. His research interests include analog and digital controller designs for power switching converters, and power system optimization.

UMAR FAROOQ received the B.Sc. and M.Sc. degrees in electrical engineering from the University of Engineering and Technology, Lahore, Pakistan, in 2004 and 2011, respectively, and the Ph.D. degree in electrical engineering from Dalhousie University, Canada, in 2018. While employed at University of the Punjab, Lahore, he taught a number of junior- and senior-level courses to the undergrad students. He also established the Society of Engineering Excellence at the department to promote research activities among the undergrad students with the generous support of the Vice-Chancellor, Prof. M. Kamran. He also supervised more than 30 senior year design projects and the students in various technical design contests, including the hardware projects exhibition, microcontroller interfacing, circuit designing, technical paper arranged by IEEE, IET, ACM, and other society chapters in Pakistan, and won more than 75 awards in these contests for University of the Punjab, in a period of four years (2008–2012). He has published a number of papers in peer-reviewed international conferences and journals. His research interests include the application of intelligent control techniques to problems in robotics, biomedical engineering, power electronics, and power systems. He was a recipient of the 2017 Dalhousie Faculty of Engineering Excellence Award and the 2017 and 2018 Nova Scotia Graduate Scholar Awards.

MUHAMMAD NAEEM SHEHZAD received the bachelor's degree in electrical engineering from the University of Engineering and Technology, Lahore, Pakistan, in 2004, the master's degree in embedded computer science and production systems from the École Centrale de Nantes, France, in 2009, and the Ph.D. degree in overhead control in global scheduling algorithms in real-time multiprocessor systems from the École Polytech de Nantes, France, in 2013. He is in involved in the development of scheduling algorithms for real-time embedded systems. He is currently with the Department of Electrical and Computer Engineering, COMSATS University Islamabad, Lahore.